BIPHASIC CALCIUM PHOSPHATE SCAFFOLDS DERIVED FROM HYDROTHERMALLY SYNTHESIZED POWDERS

Ana S. Neto, José M. F. Ferreira

Department of Materials and Ceramic Engineering, CICECO, University of Aveiro, Aveiro, Portugal

Abstract

Biphasic calcium phosphate (BCP) scaffolds were successfully produced by robocasting. The BCP powder was prepared by hydrothermal synthesis (150 °C for 4 h) and calcined at 1000 °C. The as-obtained powder was milled to obtain a suitable particle size distribution (PSD) for optimizing the rheological properties of the suspensions and pastes prepared thereof. Scaffolds with different pore dimensions (300×300, 500×500, 250×500 and 300×600 µm) were prepared by extruding the pastes through 410 µm diameter nozzles. The green scaffolds were dried and posteriorly sintered at 1100 °C. The compressive strength of the sintered scaffolds was well within the range of the mechanical properties reported from cancellous bone, being intrinsically related with the particle size distribution. Moreover, the obtained scaffolds demonstrated to have good biomineralization ability. The obtained scaffolds by robocasting revealed to possess promising features for their applications in bone regeneration and tissue engineering.

Keywords

biphasic calcium phosphates, hydrothermal synthesis, robocasting

Introduction

Currently, with the increase of life expectancy and aging population, there is a higher incidence of osteoporosis, tumor and fractures and hence a significantly increased need for bone reconstruction. The gold standard still relies on autografts. However, they are also associated with a donor site morbidity and limited available. In alternative, allografts can be used, but they are associated with risks of infection and high non-union rate to the host tissue [1]. Hence, bone tissue engineering has been explored as a promising alternative to harvesting and implantation of autografts and allografts. It involves the use of porous three-dimensional (3D) scaffolds that act as temporary supports for cell adhesion, proliferation and differentiation inducing the formation of new tissues [2, 3].

Calcium phosphate (CaP) biomaterials represent one of the most interesting materials due to their similarity to the mineral component of the bone, ensuring that they are biocompatible, non-toxic and not recognize as foreign materials. Hydroxyapatite (HA) and β-tricalcium phosphate (β-TCP) are two of the most used CaP. The CaP properties can be optimized by the combination of a more stable phase, HA, with a more soluble phase, β-TCP, forming BCP materials with a controlled bioactivity and a balance between resorption and solubilization that are beneficial for bone development [4].

Several aspects should be taken into consideration while designing a scaffold for bone tissue engineering. Apart from being biocompatible and biodegradable, the scaffolds should have an interconnected porous structure that allows cells adhesion and proliferation, but also vascularization for a subsequent bone growth. Moreover, the mechanical properties should match with the ones of the bone and be suitable during the remodeling process [5]. The conventional porous scaffolds fabrication techniques do not allow to have the control over the pore size, geometry, spatial distribution and interconnectivity. These drawbacks can be overcome using additive manufacturing techniques (AM) such as robocasting. These AM techniques enable the creation of 3D layer-by-layer structures from a computer-aided design (CAD) file and, consequently, have scaffolds with a precise control of the internal architecture, where there is no need of a subsequent machining [6, 7].

With this in mind, the aim of the present work is to synthesize the BCP powder through a hydrothermal reaction and posteriorly use it to prepare an ink with suitable viscoelastic properties for the fabrication of porous structures by additive manufacturing. Scaffolds with different pore sizes will be produced by robocasting using the optimized inks.

Lekar a technika – Clinician and Technology 2018, vol. 48(3), pp. 77–83
ISSN 0301-5491 (Print), ISSN 2336-5552 (Online)

Material and Methods

Synthesis of BCP powder

The BCP powder was prepared by hydrothermal synthesis. For this, calcium nitrate tetrahydrate [$Ca(NO_3)_2{\cdot}4H_2O$, Panreac AppliChem, Spain] was used as precursor for Ca. The phosphorous precursor was diammonium hydrogen phosphate [$(NH_4)_2HPO_4$, Panreac AppliChem, Spain]. The precursor salts were separately dissolved. 0.5 M of urea [$(NH_2)_2CO$, Riedel-de Haën, Germany] was added and to the P solution. At elevated temperatures urea decomposes and forms carbon dioxide and aqueous ammonia, which generates a gradual increase of the reaction pH to values wherein HA become thermodynamically more stable [8]. The precursors' concentrations were selected in order to have an initial Ca/P molar ratio equal to 1.57.

The phosphorous solution was added to the calcium solution under stirring and the cloudy mixture was then transferred to a stainless steel autoclave. The hydrothermal heat treatment temperature was set at 150 °C with a heating rate of about 1 ºC·min^{-1} and a dwelling time of 4 h at the maximum temperature to accomplish the hydrothermal reaction, followed by natural cooling to room temperature.

After cooling, the suspension was poured out from the autoclave, filtrated and then dried at 100 °C. The obtained powder was calcined at 1000 °C using a heating rate of 3 °C·min^{-1} and dwelling time of 2 h.

Characterization of BCP powder

The crystalline phases were identified by X-ray powder diffraction (XRD, Rigaku Geigerflex D/Max-Serie C) using Cu Kα radiation (λ = 1.5406 Å) generated at 40 mA and 45 kV. Data were obtained in the 2θ range of 10-80° using a step size of 0.0130°. The phase identification was performed by comparing the obtained XRD patterns with the standards compiled by the Joint Committee on Powder Diffraction Standards (JCPDS). The files utilized were: HA (ICDD PDF 04-015-7245) and β-TCP (ICDD PDF 04-006-9376).

A particle size analyzer (COULTER LS230, UK) with Fraunhofer optical model was used to obtain the particle size and the particle size distribution.

Optimization of robocasting ink

In order to select the most suitable dispersant addition, aqueous suspensions with a fixed volume fraction of 50 vol.% of the powder were prepared with different added amounts (0.4–1.0 wt.%) of ammonium polycarbonate dispersing agent (Targon 1128, BK Ladenburg, Germany). After selecting the optimal amount of dispersant, highly concentrated aqueous suspensions up to 58 vol.% solids were then prepared and used to study the effects of different added amounts (1–2 wt.%) of binder (hydroxypropyl methylcellulose, HPMC, Sigma-Aldrich) on the rheological properties of the suspensions. The role of the binder is to increase the apparent viscosity and present particle segregation under shear, and also to enhance the green strength of the green scaffolds. A final step of the ink preparation involves the addition of a cationic jellifying agent, polyethylenimine (PEI, 50% w/v in water, Sigma-Aldrich). Different amounts (0.1–0.3 wt.%) of PEI were added in order to adjust the viscoelastic properties to the suitable level for extrusion through the fine nozzles. After the addition of each processing additive, the ink was placed in a planetary centrifugal mixer (ARE-250, Thinky Corp., Tokyo, Japan) to achieve a good homogeneity of the mixture.

The rheological behavior of the inks was assessed by using a Kinexus Pro$^+$ Rheometer (Malvern, USA). The flowing behavior was assessed using a cone plate sensor system (4°/40 mm) and 150 µm gap size. The curves of apparent viscosity *versus* shear rate were registered in the viscometry mode. The viscoelastic behavior was assessed under the oscillatory mode by using a plate and plate sensor (20 mm) and a 1 mm gap size. It was registered the elastic modulus (G') *versus* applied complex shear stress.

Production of scaffolds by robocasting

The optimized ink was extruded through cylindrical metallic nozzles with an inner diameter of 410 µm using a printing speed of 10 mm·s^{-1}. Each printed structure consisted of 9 scaffolds of approximately 3×3×3 mm^3. To prevent a non-uniform drying of the structures, the layer-by-layer deposition was carried out within a paraffin oil bath. Scaffolds with different porosities of 300×300, 500×500, 250×500 and 300×600 µm were produced. The as-obtained scaffolds were dried in air at room temperature and then subjected to a heat treatment with a slow heating rate of 1 °C·min^{-1} up to 400 °C for 1 h to burn the organic additives. Subsequently, the scaffolds were sintered with a heating rate of 3 °C·min^{-1} at 1100 °C for 2 h.

Microstructure and mechanical characterization

The microstructure of the sintered scaffolds was observed by scanning electron microscopy (SEM, Hitachi SU-70, Hitachi High-Technologies Europe, GmbH, Germany) with an acceleration voltage of 25 kV and beam current of 10 µA.

For assessing the mechanical properties, the sintered scaffolds were subjected to uniaxial compressive strength measurements using a universal testing machine (AG-IS10kN, Shimadzu, Kyoto, Japan). The scaffolds were subjected to a 200 N maximum load at a constant speed of 0.5 mm·min^{-1} in ambient conditions.

In vitro biomineralization

The scaffolds with pore dimensions of 300×300 were used to study the *in vitro* biomineralization capability.

Lekar a technika – Clinician and Technology 2018, vol. 48(3), pp. 77–83
ISSN 0301-5491 (Print), ISSN 2336-5552 (Online)

SBF was prepared accordingly to the standard ISO 23317:2014(E) protocol [9] and it was used a unifying standard area (S_A) of 0.5 $cm^2 \cdot ml^{-1}$ of SBF solution resent proposed elsewhere [10]. Briefly, the scaffolds were immersed in SBF at 37 °C and sampling took place after 7 and 14 days. After each immersion time, the samples were collected from the SBF solution and rinsed with distilled water and placed in a silica desiccation. The morphology of the dried samples was observed by SEM, under the same conditions as reported above.

Results and discussion

Synthesis and characterization of BCP powder

Wet chemical precipitation [11, 12] and sol-gel [13, 14] are two of the most used methods to produce CaP powders for a further production of scaffolds by robocasting. In this work, hydrothermal method was explored for the production of a BCP powder. In this technique, the reaction between the chemicals occurs at elevated temperatures and pressures, normally above the boiling temperature of water and inside an autoclave [15]. The success of the hydrothermal reaction is dependent on different factors, namely the temperature and pH [16, 17]. The increase of the temperature of reaction result in the formation of HA, as the dominant phase [17]. The reaction pH directly influences the growth of HA crystals. In order to work under optimal pH conditions, urea is being added as a precipitation agent instead of ammonia [16] since it hydrolyzes in a homogeneous way, enabling the nucleation and growth of HA crystals in moderated supersaturation conditions [8]. In most of the works that approach a urea-assisted reaction for the HA synthesis it was used with a urea concentration of 0.5 M and a temperature of reaction of 90 °C and this temperature was maintained for different periods of time from 3 to 10 days [8, 16, 18]. Moreover, Ca/P ratio increases with increasing pH, as a consequence of the addition of urea, or with increasing temperature. Under this regard, it is required the use of a Ca/P molar ratio smaller than the stochiometric value [16].

In this work, it was maintained a urea concentration of 0.5 M, but it was tested a different temperature and dwelling time conditions of 150 °C and 4 h, respectively. Under these conditions, a BCP powder was successfully obtained as illustrated in Fig. 1. As a matter of fact, the observed XRD patterns closely resemble those of HA (ICDD PDF 04-015-7245) and β-TCP (ICDD PDF 04-006-9376) phases, respectively.

A suitable PSD is of paramount importance for ceramic processing as it enables a good packing of the particles. This requirement is especially relevant when colloidal techniques are adopted, as the rheological properties of the suspensions and the maximum achievable solids loadings are strongly affected by particle size and PSD [19].

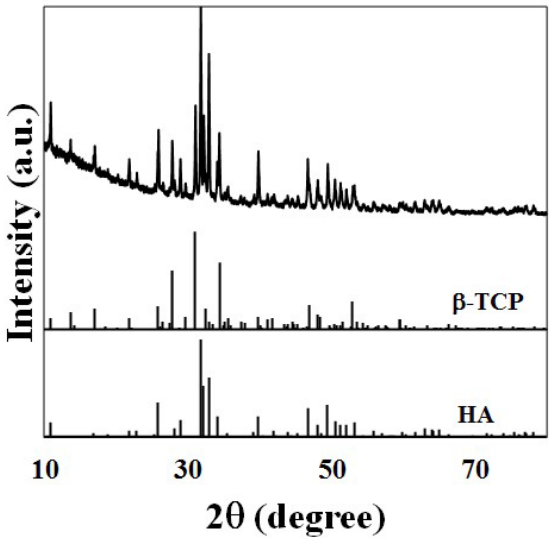

Fig. 1: XRD pattern of the BCP powder calcined at 1000 °C. The standard ICDD PDF 04-006-9376 and 04-015-7245 of pure β-TCP and HA, respectively, are also present for comparison purposes.

The obtained PSD curve is displayed in Fig. 2. The average particle size of the powder was 1.29 µm. The deconvolution of the overall PSD curve enables to observe that it consists of three main populations. The finest population is centered at around 0.55 µm and the most significant particle population is the intermediate sized centered at around 2.4 µm. The third population represents insufficiently destroyed particle agglomerates.

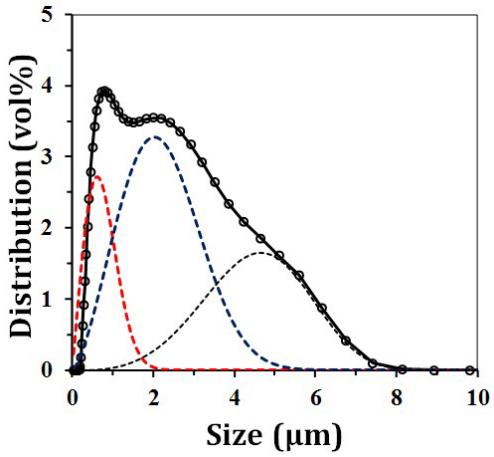

Fig. 2: Particle size distribution of BCP powder.

Optimization of robocasting ink

In a first step, aqueous suspensions with 50 vol.% were prepared containing only the dispersant (Targon 1128) to evaluate the effects of different dispersant

concentrations. The flow curves displayed in Fig. 3a exhibit shear thinning behaviors characteristic of well dispersed suspensions that are not likely to undergo shear induced coagulation. This is an important feature for systems that will be subjected to relatively high shear rates like robocasting. Another aim of these preliminary dispersion tests was to find out the most suitable content of dispersant that allows minimizing the apparent viscosity of the suspension. It can be observed that for all the compositions, the increase of the Targon 1128 cause unwanted contrary effects and, therefore, the amount of dispersant chosen for all the compositions is 0.4 wt.%.

With the optimized amount of dispersant, different solid volume fractions were tested in order to find out the maximum achievable solid loadings. The resulting flow curves shown in Fig. 3b demonstrate that for a given shear rate, the apparent viscosity continuously increases with increasing solids volume fraction. Suspensions with solid loading higher than 58 vol.% revealed to be less reliable, exhibiting non-reproducible rheological behaviors.

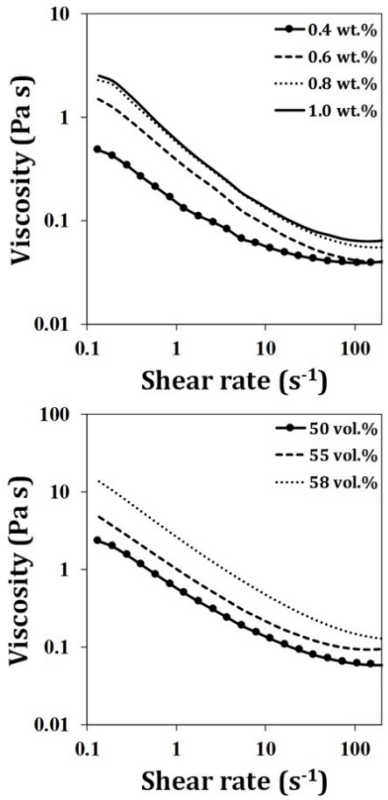

Fig. 3: Viscosity as a function of shear rate for the suspensions prepared with (a) different amounts of dispersant and with (b) different solid loadings from BCP powder.

Therefore, 58 vol.% corresponds to the maximum achievable solid loading using this BCP powder. Such relatively high solid loading may be due to an effective destruction of the particle agglomerates during dry milling and the achievement of suitable particle size distribution that confers to the suspensions the desired shear-thinning behavior.

Once a high solid loading suspension with suitable flowing ability has been obtained, it is necessary to increase its intrinsic viscosity to avoid particle segregation under shear and accentuate the shear thinning behavior. This goal can be achieved by adding a viscosifier agent such as the HMPC. Two different amounts of HPMC (1 and 2 wt.%) were tested and Fig. 4 compares the flow curves without and with these two added amounts of HPMC. A gradual increase in apparent viscosity with incremental amounts of HPMC is evident for all systems. The most pronounced upshift of the viscosity is registered with the addition of 2 wt.%. Therefore, this concentration was selected. These results are in good agreement with the role of the vicosifier agent.

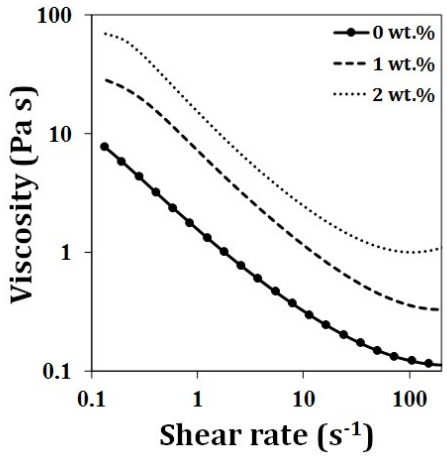

Fig. 4: Viscosity as a function of shear rate for the suspensions prepared with different amounts of HPMC from BCP powder.

The last step of ink preparation involves the addition of a coagulating agent to adjust the viscoelastic properties of the paste to enable shape retention after extruding. This was achieved by studying the influence of PEI content on the rheological properties (Fig. 5).

The results presented in Fig. 5 confirm that small added amounts of PEI cause strong changes on rheological properties. When assessed under rotation mode, the flow curves of the different compositions show drastic upshifts with increasing PEI contents (Fig. 5a). These changes mean that the electrostatic double layers and the steric hindrances promoted by the polyelectrolyte chains adsorbed at the surface of the particles tend to gradually collapse upon adding the cationic additive, coagulation the system. The coagulation effects of PEI are also very evident upon assessing the viscoelastic properties under the oscillatory mode.

The plots of elastic modulus (G') *versus* applied complex shear stress are displayed in Fig. 5b and are

Lekar a technika – Clinician and Technology 2018, vol. 48(3), pp. 77–83
ISSN 0301-5491 (Print), ISSN 2336-5552 (Online)

used to study the shape stability of the extruded filaments. It can be observed that the incorporation of PEI significantly enlarged the linear viscoelastic region and increased the elastic modulus (G'). The paste containing 0.3 wt.% of PEI exhibit the most extended linear viscoelastic region and the highest G' values, being an indicative that the final ink will be mechanically stable and able to support their own weight during deposition.

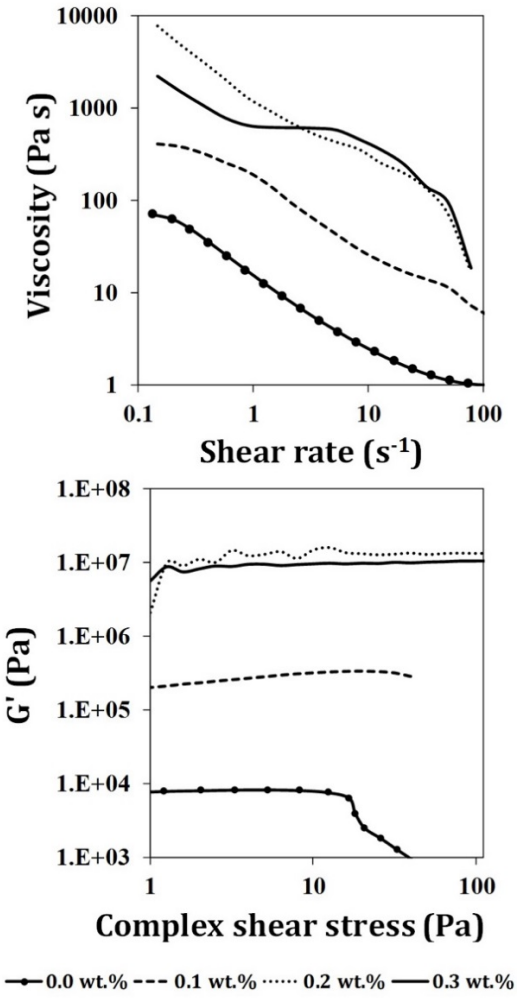

Fig. 5: Effects of the addition of different amount of PEI on the rheological behavior of the BCP ink: (a) Viscosity as a function of shear rate; (b) Elastic modules measured under oscillatory amplitude sweeps.

Due to the incorporation of HPMC and PEI, which are added as aqueous solutions, the solid loading of the final ink decreased from 58 vol.% to 51 vol.%. This concentration of solids is enough high to enable a good dimensional control of the deposited porous structures over the drying and sintering processing steps. For example, even assuming that full densification would occur upon sintering, the overall linear shrinkage undergone by the scaffolds would be around 16%.

Microstructure and mechanical characterization

Scanning electron micrographs of the side views of the scaffolds prepared with the optimized ink are shown in Fig. 6. a good adhesion between the adjacent layers can be inferred from these images. Further, the rods exhibit a relative straight shape.

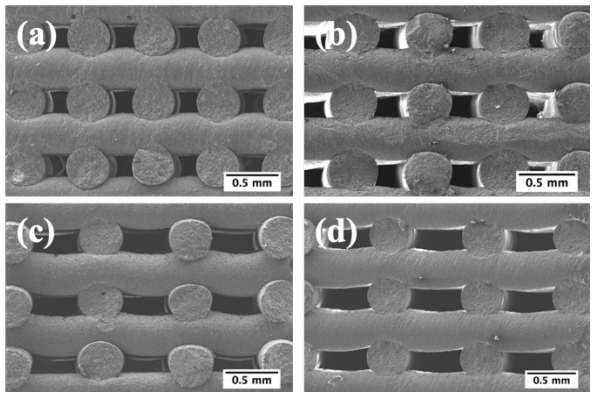

Fig. 6: SEM micrographs of the internal micro-structure with different pore sizes: (a) 250, (b) 300, (c) 500 and (d) 600 µm after sintering at 1100 °C.

The microstructures of the sintered rods are displayed in Fig. 7. The rods exhibit appreciable and similar fractions of microporosity left after sintering. Scaffolds with macroporosity are required for bone ingrowth as it allows cell infiltration and a subsequent formation of extracellular matrix as well as the diffusion of oxygen and nutrients and the removal of waste products. However, it is important to highlight that both micro and nanoporosity play crucial roles on cell adhesion, biomineralization and on *in vivo* osteointegration [20, 21]. Under this regard, the obtained scaffolds seem to meet the essential requirements for bone regeneration and tissue engineering applications.

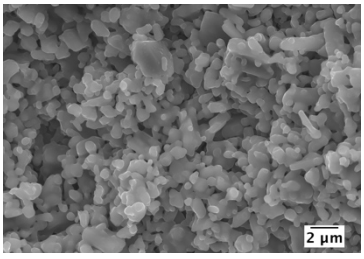

Fig. 7: Microstructure of the sintered rods.

The obtained values of compressive strength presented in Fig. 8 shown an overall decreasing trend with increasing pore size and porosity fraction. This trend is more than expected considering that mechanical properties are known to decrease when the fraction of solid material decreases [5, 22–25]. Accordingly, it is not surprising that better results were achieved for scaffolds with smaller pore dimensions (300×300 µm)

with a compressive strength of 6.58 ± 0.51 MPa. Lower values of compressive strength were achieved with higher pore dimensions, namely 3.46 ± 0.20 and 3.64 ± 0.08 MPa for the scaffolds with a pore dimension of 300×600 and 500×500 µm, respectively.

In addition, it is important to highlight that the compressive strength values measured for all the tested scaffolds are well within the range of compressive strength values (2–12 MPa) reported for cancellous bone [26].

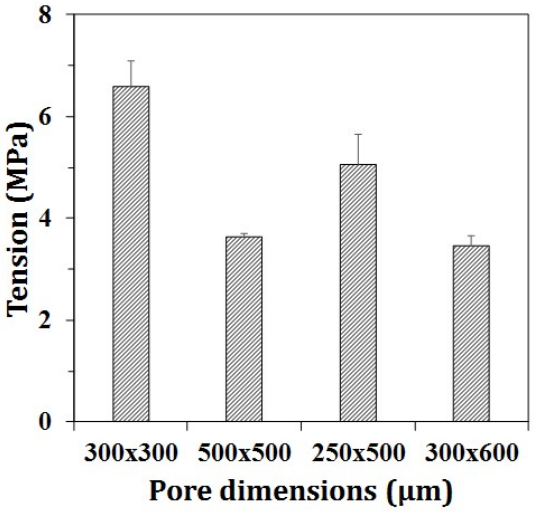

Fig. 8: Compressive strength of sintered scaffolds with different pore sizes.

In vitro biomineralization

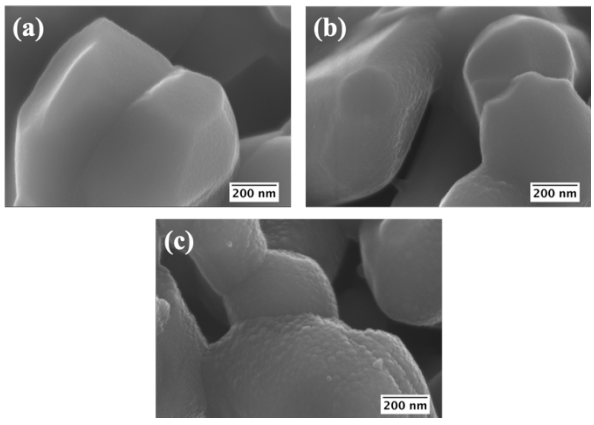

Fig. 9: SEM micrographs of the surface of scaffolds after immersion in SBF for (a) 0 h; (b) 7 days and (c) 14 days.

The morphological effects derived from the changes undergone by the scaffolds during the in vitro biomineralization tests are shown in Fig. 9. Before the immersion in SBF solution, the scaffolds exhibited grains with smooth surfaces, which then became gradually rougher upon increasing the duration of the immersion period in SBF. The changes already well noticed after 7 days of increasing, became more expressive after 14 days. This occurs due to the dissolution-precipitation reactions that occur at the solid/liquid interface.

Conclusion

Scaffolds with different porosities were successfully obtained by robocasting from BCP powder. An efficient destruction of particle agglomerates is essential for allowing the particles packing well to confer to the resulting suspensions a shear thinning behavior to prevent clogging of the extrusion fine nozzles. Further, adding the optimal amounts of processing additives is another fundamental requirement for the printing ability of the pastes. The obtained scaffolds possess compressive strength values that are within those reported for the trabecular bone and exhibit a good *in vitro* biomineralization. Overall, the obtained scaffolds revealed to be promising for bone regeneration and bone tissue engineering applications.

Acknowledgement

This work was developed within the scope of the project CICECO-Aveiro Institute of Materials, POCI-01-0145-FEDER-007679 (FCT Ref. UID /CTM /50011/2013), University of Aveiro, financed by national funds through the FCT/MEC, Portugal, and when appropriate co-financed by FEDER under the PT2020 Partnership Agreement. Ana S. Neto is grateful to AdvaMTech, the PhD Program on Advanced Materials and Processing for the PhD grant, PD/BD/114132/2015, founded by the Portuguese Foundation for Science and Technology (FCT).

References

[1] Oryan, A., Alidadi, S., Moshiri, A., Maffulli, N.: *Bone regenerative medicine: classic options, novel strategies, and future directions.* J. Orthop. Surg. Res., 2014, vol. 9, pp. 1–18.

[2] Mouriño, V., Boccaccini, A. R.: *Bone tissue engineering therapeutics: controlled drug delivery in three-dimensional scaffolds.* J. R. Soc. Interface, 2010, vol. 7, no. 43, pp. 209–227.

[3] Perez, R. A., Seo, S. J., Won, J. E., Lee, E. J., Jang, J. H., Knowles, J. C., Kim, H. W.: *Therapeutically relevant aspects in bone repair and regeneration.* Mater. Today, 2015, vol. 18, no. 10, pp. 573–589.

[4] Lobo, S. E., Arinzeh, T. L.: *Biphasic calcium phosphate ceramics for bone regeneration and tissue engineering applications.* Materials, 2010, vol. 3, no. 2, pp. 815–826.

[5] O'Brien, F. J.: *Biomaterials & scaffolds for tissue engineering.* Mater. Today, 2011, vol. 14, no. 3, pp. 88–95.

[6] Bose, S., Vahabzadeh, S., Bandyopadhyay, A.: *Bone tissue engineering using 3D printing.* Mater. Today, 2013, vol. 16, no. 12, pp. 496–504.

[7] Henkel, J., Woodruff, M. A., Epari, D. R., Steck, R., Glatt, V., Dickinson, I. C., Choong, P. F. M., Schuetz, M. A., Hutmacher, D. W.: *Bone Regeneration Based on Tissue Engineering Conceptions — A 21st Century Perspective.* Bone Res., 2013, vol. 1, no. 3, pp. 216–248.

[8] Gupta, H. S., Guitia, F.: *An effective morphology control of hydroxyapatite crystal via hydrothermal synthesis.* Cryst. Growth Des., 2009, vol. 9, pp. 466–474.

[9] International Standard ISO 23317:2014(E). *Implants for surgery - In vitro evaluation for apatite-forming ability of implant materials.* 2014.

[10] Popa, A. C., Stan, G. E., Husanu, M. A., Mercioniu, I., Santos, L. F., Fernandes, H. R., Ferreira, J. M. F.: *Bioglass implant-coating interactions in synthetic physiological fluids with varying degrees of biomimicry.* Int. J. Nanomedicine., 2017, vol. 12, pp. 638–707.

[11] Marques, C. F., Perera, F. H., Marote, A., Ferreira, S., Vieira, S. I., Olhero, S., Miranda, P., Ferreira, J. M. F.: *Biphasic calcium phosphate scaffolds fabricated by direct write assembly: Mechanical, anti-microbial and osteoblastic properties.* J. Eur. Ceram. Soc., 2017, vol. 37, no. 1, pp. 359–368.

[12] Zou, F., Zhao, N., Fu, X., Diao, J., Ma, Y., Cao, X., Wan, S., Zhong, S., Wang, Y.: *Enhanced osteogenic differentiation and biomineralization in mouse mesenchymal stromal cells on a β-TCP robocast scaffold modified with collagen nanofibers.* RSC Adv., 2016, vol. 6, no. 28, pp. 23588–23598.

[13] Houmard, M., Fu, Q., Saiz, E., Tomsia, A. P.: *Sol-gel method to fabricate CaP scaffolds by robocasting for tissue engineering.* J. Mater. Sci. Mater. Med., 2012, vol. 23, no. 4, pp. 921–930.

[14] Miranda, M., Fernández, A., Saiz, E., Tomsia, A. P., Torrecillas, R.: *Application of new forming and sintering techniques to obtain hydroxyapatite and β-TCP nanostructured composites.* Int. J. Mater. Res., 2010, vol. 101, no. 1, pp. 117–121.

[15] Sadat-Shojai, M., Khorasani, M. T., Dinpanah-Khoshdargi, E., Jamshidi, A.: *Synthesis methods for nanosized hydroxyapatite with diverse structures.* 2013, vol. 9, no. 8, pp. 7591–7621.

[16] Sadat-Shojai, M., Atai, M., Nodehi, A.: *Design of Experiments (DOE) for the Optimization of Hydrothermal Synthesis of Hydroxyapatite Nanoparticles.* 2011, vol. 22, no. 3, pp. 571–582.

[17] Sadat-Shojai, M., Khorasani, M.-T., Jamshidi, A.: *Hydrothermal processing of hydroxyapatite nanoparticles—A Taguchi experimental design approach.* J. Cryst. Growth. 2012, vol. 361, pp. 73–84.

[18] Mohammadi, Z., Sheikh-Mehdi Mesgar, A., Rasouli-Disfani, F.: *Preparation and characterization of single phase, biphasic and triphasic calcium phosphate whisker-like fibers by homogenous precipitation using urea.* Ceram. Int, 2016, vol. 42, no. 6, pp. 6955–6961.

[19] Lemos, A. F., Santos, J. D., Ferreira, J. M. F.: *Influence of characteristics of starting hydroxyapatite powders and of deagglomeration procedure, on rheological behaviour of HA suspensions.* Mater. Sci. Forum, 2004, vol. 455–456, pp. 361–365.

[20] Bose, S., Roy, M., Bandyopadhyay, A.: *Recent advances in bone tissue engineering scaffolds.* Trends Biotechnol., 2012, vol. 30, no. 10, pp. 546–554.

[21] Tang, W., Lin, D., Yu, Y., Niu, H., Guo, H., Yuan, Y., Liu, C.: *Bioinspired trimodal macro/micro/nano-porous scaffolds loading rhBMP-2 for complete regeneration of critical size bone defect.* Acta Biomater., 2016, vol. 32, pp. 309–323.

[22] Lee, H., Jang, T. S., Song, J., Kim, H. E., Do Jung, H.: *The production of porous hydroxyapatite scaffolds with graded porosity by sequential freeze-casting.* Materials, 2017, vol. 10, no. 4, pp. 1–12.

[23] An, J., Teoh, J. E. M., Suntornnond, R., Chua, C. K.: *Design and 3D Printing of Scaffolds and Tissues.* Engineering, 2015, vol. 1, no. 2, pp. 261–268.

[24] Sabree, I., Gough, J. E., Derby, B.: *Mechanical properties of porous ceramic scaffolds: Influence of internal dimensions.* Ceram. Int., 2015, vol. 41, no. 7, pp. 8425–8432.

[25] Bose, S., Vahabzadeh, S., Bandyopadhyay, A.: *Bone tissue engineering using 3D printing.* Mater. Today, 2013, vol. 16, no. 12, pp. 496–504.

[26] Carter, D. R., Schwab, G. H., Spengler, D. M.: *Tensile fracture of cancellous bone.* Acta Orthop. Scand., 1980, vol. 51, no. 1–6, pp. 733–741.

Ana S. Neto
Department of Materials and Ceramic Engineering
CICECO, University of Aveiro
Campus Santiago, 3810-193 Aveiro, Portugal

E-mail: sofia.neto@ua.pt